# Optical Transition Probability of $Sm^{3+}$ Ions in a Polymer Optical Fibre *

ZHENG Zhi-Qiang(郑志强)[1,3], LIANG Hao(梁浩)[2], MING Hai(明海)[1**], ZHANG Qi-Jin(张其锦)[2], HAN Xin-Hai(韩新海)[1], WANG Guan-Zhong(王冠中)[1], XIE Jian-Ping(谢建平)[1]

[1]*Department of Physics, University of Science and Technology of China, Hefei 230026*
[2]*Structure Research Laboratory and Department of Material Science and Engineering, University of Science and Technology of China, Hefei 230026*
[3]*Department of Physics, Fujian Normal University, Fuzhou 350007*

(Received 14 July 2003)

*We investigate optical absorption and emission spectra of $Sm^{3+}$ ions in $Sm(DBM)_3Phen$-doped polymethyl methacrylate (PMMA). Based on the Judd–Ofelt theory, the optical intensity parameters are calculated to be $\Omega_2 = 13.76 \times 10^{-20}\,cm^2$, $\Omega_4 = 3.41 \times 10^{-20}\,cm^2$, $\Omega_6 = 4.01 \times 10^{-20}\,cm^2$ from the absorption spectrum of $Sm(DBM)_3Phen$-doped polymethyl methacrylate. The optical intensity parameters have been used to calculate the total radiative transition rate ($676.57\,s^{-1}$) and radiative lifetime ($1478\,\mu s$) of the $^4G_{5/2}$ exciting state. The stimulated emission cross-sections $\sigma_{ij}$ and the fluorescence branch ratios for the $^4G_{5/2} \to {}^6F_{J'}$ and $^4G_{5/2} \to {}^6H_{J'}$ transitions are also evaluated. The analysis reveals that $Sm(DBM)_3Phen$-doped PMMA is promising for applications in rare-earth-doped polymer devices.*

*PACS: 32. 70. Cs, 42. 70. Jk, 42. 81. Qb*

There has been an increasing interest in researching efficient new materials for polymer optical fibre (POF) devices because of their applications in optical communication systems and optical sensors, especially in local networks. In recent years, great effort has been taken to rare-earth-doped POFs. $Nd^{3+}$, $Eu^{3+}$, $Pr^{3+}$ and $Er^{3+}$ ions were doped into POFs.[1−6] Amplified spontaneous emission (ASE) was found in $Nd^{3+}$-doped POFs [5] and in $Eu^{3+}$-doped graded-index POFs.[6] This indicates that the rare-earth-doped POF has the possibility to make the POF amplifier or POF laser. To evaluate the potential of rare-earth-doped POFs, it is essential to study the radiative properties of the rare-earth organic complexes. As usual, the radiation properties of trivalent rare-earth ions in host matrix can be predicted from optical absorption measurement and by using the Judd–Ofelt theory.[7−12] In Ref. [4] the authors used the fluorescence spectrum to obtain the Judd–Ofelt parameters of $Eu(DBM)_3Phen$-doped PMMA because only a few absorption transitions are observed with good intensities in $Eu(DBM)_3Phen$-doped PMMA and only a few equations for the least-squares fitting can be provided. The 613-nm emission line is most important of the lines in $Eu(DBM)_3Phen$-doped PMMA.

In this Letter, we analyse the absorption and the fluorescence spectra of $Sm(DBM)_3Phen$-doped polymethyl methacrylate (PMMA) developed in our laboratory. We obtained the electric-dipole line strengths and optical intensity parameters of $Sm^{3+}$ in $Sm(DBM)_3Phen$-doped PMMA as calculated by the Judd–Ofelt theory using the values of the absorption spectrum of $Sm(DBM)_3Phen$-doped PMMA. The calculated values of the optical intensity parameters were utilized in evaluating the various radiative parameters such as the radiative lifetime of the $^4G_{5/2}$ excited state, the stimulated emission cross-sections and the fluorescence branch ratios for the $^4G_{5/2} \to {}^6F_{J'}$ and $^4G_{5/2} \to {}^6H_{J'}$ transitions. The 648-nm emission line is most important among the emission lines of $Sm(DBM)_3Phen$-doped PMMA, which the centre of the communication window of methyl methacrylate-based POF is about 650 nm in wavelength.

The fabrication of $Sm(DBM)_3Phen$-doped PMMA include two steps. One is the synthesis of $Sm(DBM)_3Phen$,[13] and the other is the polymerization of $Sm(DBM)_3Phen$ and methyl methacrylate (MMA). The $Sm(DBM)_3Phen$-doped PMMA and $Sm(DBM)_3Phen$-doped polymer optical fibres have been fabricated using the same method as described in our previous paper.[4] To our knowledge, the $Sm^{3+}$-doped polymer optical fibre was successfully fabricated for the first time. Figure 1 shows the absorption spectrum of $Sm(DBM)_3Phen$-doped PMMA(1cm thick slice) which measured by UV-VIS-NIR spectrophotometer (PerkinElmer Lambda 900). The concentration of $Sm^{3+}$ in $Sm(DBM)_3Phen$-doped PMMA is 0.5 wt.%. The band positions in the absorption spectrum are shown in Table 1. Figure 2 shows the fluorescence spectrum of $Sm(DBM)_3Phen$-doped PMMA

* Supported by the National Natural Science Foundation of China under Grant Nos 90201013 and 90201016, and the Natural Science Foundation of Fujian Province under Grant No A0110012, and the Educational Foundation of Fujian Province under Grant No JA02169.

** To whom correspondence should be addressed. Email: minghai@ustc.edu.cn

©2004 Chinese Physical Society and IOP Publishing Ltd

which measured by a fluorescence spectrophotometer (Shimadzu RF-5301) at excitation of 476 nm using a xenon lamp. The three emission peaks correspond to the $^4G_{5/2} \rightarrow {}^6H_{9/2}$ (648 nm), $^4G_{5/2} \rightarrow {}^6H_{7/2}$ (601 nm) and $^4G_{5/2} \rightarrow {}^6H_{5/2}$ (566 nm) transitions.

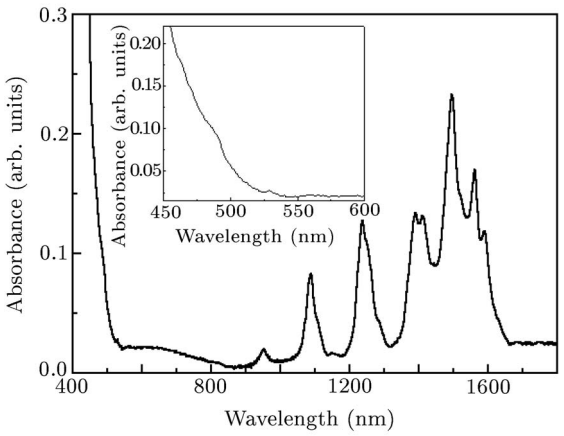



**Fig. 1.** Absorption spectrum of $Sm(DBM)_3Phen$-doped PMMA. Inset: enlarged profile of the absorption spectrum from 450 nm to 600 nm wavelength.

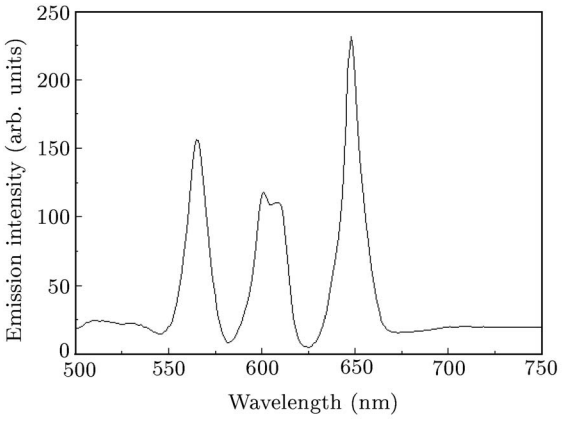



**Fig. 2.** Fluorescence spectrum of $Sm(DBM)_3Phen$-doped PMMA.

Table 1. Measured and calculated line strengths of $Sm^{3+}$ in $Sm(DBM)_3Phen$-doped PMMA (all the transitions are from $^6H_{5/2}$).

| Level | $\lambda$ (nm) | $S_{\rm expt}$ ($10^{-20}$cm$^2$) | $S_{\rm calc}$ ($10^{-20}$cm$^2$) |
|---|---|---|---|
| $^4I_{13/2}$ | 465 | 0.0311 | 0.1016 |
| $^4I_{9/2}$, $^4M_{15/2}$ | 491 | 0.0894 | 0.1606 |
| $^4F_{3/2}$ | 529 | 0.0203 | 0.0041 |
| $^6F_{11/2}$ | 950 | 0.2292 | 0.2080 |
| $^6F_{9/2}$ | 1088 | 1.2775 | 1.4379 |
| $^6F_{7/2}$ | 1237 | 2.3702 | 2.2408 |
| $^6F_{5/2}$ | 1389 | 1.3699 | 1.4262 |
| $^6F_{3/2}$, $^6F_{1/2}$, $^6H_{15/2}$ | 1539 | 5.1429 | 5.1377 |
| $\rm rms(\Delta S) = 0.1062 \times 10^{-20} cm^2$ | | | |

The experimental line strength of an electric-dipole transition $S_{\rm expt}$ can be calculated from the following formula:[14]

$$\int k(\lambda)d\lambda = \rho\frac{8\pi^3e^2\bar{\lambda}}{3ch(2J+1)}\frac{1}{n}\left[\frac{(n^2+2)^2}{9}\right]S_{\rm expt}, \quad (1)$$

where $k(\lambda)$ is the absorption coefficient at wavelength $\lambda$; $\rho$ is the $Sm^{3+}$-ion concentration; $e$, $h$ and $c$ are the electron charge, the Planck constant and velocity of light, respectively; $\bar{\lambda}$ is the mean wavelength of the absorption band, $J$ is the total angular momentum of the initial level ($J = 5/2$ in $Sm^{3+}$), and $n$ is refractive index, which is 1.496 for $Sm(DBM)_3Phen$-doped PMMA.

According to the Judd–Ofelt theory, the line strength of an electric-dipole transition between initial $J$ manifold and terminal $J'$ manifold may be written in the form of [14]

$$S = \sum_{t=2,4,6} \Omega_t |\langle f^N \Psi_J \| U^{(t)} \| f^N \Psi'_{J'} \rangle|^2, \quad (2)$$

where the elements $U^{(t)}$ are the doubly reduced unit tensor operators, which can be derived from Ref. [15]; $\Omega_t$ are the optical intensity parameters, $f^N \Psi_J$ are the wavefunction of the states with $N$ electrons in $4f$ shell having total angular momentum $J$. The parameters $\Omega_2$, $\Omega_4$, and $\Omega_6$ are independent of electronic quantum numbers with the ground configuration of the $Sm^{3+}$ ion. They may be regarded as the phenomenological parameters that characterize the radiative transition probabilities within the ground configuration. Using Eq. (1) and the values of the absorption spectrum of $Sm(DBM)_3Phen$-doped PMMA, the experimental line strength $S_{\rm expt}$ for the electric dipole transition can be obtained. After $S_{\rm expt}$ is obtained, the optical intensity parameter $\Omega_t$ can be obtained by least-squares fitting of Eq. (2): $\Omega_2 = 13.76 \times 10^{-20}$ cm$^2$, $\Omega_4 = 3.41 \times 10^{-20}$ cm$^2$, $\Omega_6 = 4.01 \times 10^{-20}$cm$^2$. The large value for $\Omega_2$ indicates the presence of covalent bonding between the rare-earth ions and the surrounding ligands, it reflects the large asymmetry of the local environment at $Sm^{3+}$.

To justify the result obtained, we use the calculated $\Omega_t$ to calculate the electric-dipole line strength $S_{\rm calc}$ of the absorption bands. The experimental and corresponding calculated line strength data for $Sm(DBM)_3Phen$-doped PMMA are displayed in Table 1. The root-mean-square deviation between the experimental and calculation line strengths is calculated in the usual way,

$$\rm rms(\Delta S) = \left[\frac{(S_{expt} - S_{calc})^2}{N - M}\right]^{1/2}, \quad (3)$$

where $N$ is the number of transitions and $M$ is the number of parameters determined. The obtained rms value is rather large because the $^6H_{5/2} \rightarrow {}^6F_{3/2}$ transition is the hypersensitive transition that has the large

line strength and the $^6H_{5/2} \rightarrow {}^6F_{3/2}$, $^6H_{5/2} \rightarrow {}^6F_{1/2}$, $^6H_{5/2} \rightarrow {}^6H_{15/2}$ absorption transitions overlapped by more than 5% were treated as a single experimental point in the fitting calculation.

The radiative transition rate $A$ from initial $J$ manifold to terminal $J'$ manifold is calculated by

$$A = \frac{64\pi^4 e^2 \nu^3}{3h(2J+1)} \frac{n(n^2+2)^2}{9} \cdot \sum_{t=2,4,6} \Omega_t |\langle f^N \Psi_j \| U^{(t)} \| f^N \Psi'_{j'} \rangle|^2, \quad (4)$$

where $\nu$ is the frequency in inverse centimetres. The radiation lifetime for the excited emission of $Sm^{3+}$ ion can be written as

$$\frac{1}{\tau_i} = \sum_j A_{ij}, \quad (5)$$

where $\tau_i$ is the total radiation lifetime of the metastable state $^4G_{5/2}$ manifold $J$. $A_{ij}$ is the radiative transition rate for transition $f^N \Psi_J \rightarrow f^N \Psi'_{J'}$. Then the fluorescence branch ratios $\beta$ are defined by

$$\beta = \frac{A_{ij}}{\sum_j A_{ij}}, \quad (6)$$

where the sum is taken over all the possible terminal manifolds. This represents the total radiation transition rate $A_T$ for radiation decay from the initial manifold. The calculated radiation lifetime $\tau_R$ of the $^4G_{5/2}$ metastable state, the radiation transition rates and fluorescence branch ratios of $^4G_{5/2} \rightarrow {}^6F_{J'}$ and $^4G_{5/2} \rightarrow {}^6H_{J'}$ are listed in Table 2.

Table 2. Calculated radiation lifetime of the $^4G_{5/2}$ metastable state, the radiative transition rates and fluorescence branch ratios of $^4G_{5/2} \rightarrow {}^6F_{J'}$ and $^4G_{5/2} \rightarrow {}^6H_{J'}$.

| $SLJ$ | $S'L'J'$ | $\lambda$ (nm) | $\langle U^{(2)} \rangle^2$ | $\langle U^{(4)} \rangle^2$ | $\langle U^{(6)} \rangle^2$ | $A$ ($s^{-1}$) | $\beta$ |
|---|---|---|---|---|---|---|---|
| $^4G_{5/2}$ | $^6F_{11/2}$ | 1460 | 0 | 0.0001 | 0.0005 | 0.4060 | 0.0006 |
| | $^6F_{9/2}$ | 1198 | 0.0018 | 0.0003 | 0.0002 | 8.3368 | 0.0123 |
| | $^6F_{7/2}$ | 1038 | 0 | 0.0017 | 0.0002 | 3.1828 | 0.0047 |
| | $^6F_{5/2}$ | 953 | 0.0072 | 0.0017 | 0 | 65.244 | 0.0964 |
| | $^6F_{3/2}$ | 908 | 0.0011 | 0.0001 | 0 | 11.141 | 0.0165 |
| | $^6H_{15/2}$ | 902 | 0 | 0 | 0.0002 | 0.5888 | 0.0009 |
| | $^6F_{1/2}$ | 893 | 0.0010 | 0 | 0 | 10.418 | 0.0154 |
| | $^6H_{13/2}$ | 795 | 0 | 0.0002 | 0.0018 | 8.4604 | 0.0125 |
| | $^6H_{11/2}$ | 708 | 0 | 0.0053 | 0.0021 | 40.215 | 0.0594 |
| | $^6H_{9/2}$ | 648 | 0.0112 | 0.0067 | 0.0020 | 348.61 | 0.5153 |
| | $^6H_{7/2}$ | 601 | 0.000 | 0.0086 | 0.0089 | 164.70 | 0.2434 |
| | $^6H_{5/2}$ | 566 | 0.0002 | 0.0007 | 0 | 15.269 | 0.0226 |
| | $A_T$ ($^4G_{5/2}$) = 676.57 $s^{-1}$, $\tau_R$ = 1478 $\mu$s | | | | | | |

It can be seen that the $^4G_{5/2} \rightarrow {}^6H_{9/2}$ transition (648 nm) is most important. The radiation lifetime of $^4G_{5/2}$ is equal to 1478 $\mu$s. This value is comparable with that of samarium-doped silica-glass systems that have been used to make fibre lasers.[16] The $^4G_{5/2}$ metastable state lifetime indicates that it is efficient for laser pumping.

With values for the radiation transition rates calculated above, along with the corresponding fluorescence spectrum (Fig. 2), the stimulated emission cross-section $\sigma_{ij}$ is given by

$$\sigma_{ij} = \frac{A_{ij} \langle \lambda \rangle^4}{8\pi^2 n^2 c \Delta\lambda}, \quad (7)$$

where $\Delta\lambda$ and $\langle \lambda \rangle$ are the effective band width and the mean wavelength of the emission transition, respectively. The calculated emission cross-sections for the fluorescence transitions are given in Table 3. It should be noted that the emission cross-section is maximum for the transition $^4G_{5/2} \rightarrow {}^6H_{9/2}$. The emission cross-section for the 648 nm transition is of the same order of magnitude as that for $Sm^{3+}$-doped silica-glass systems. The $Sm(DBM)_3Phen$-doped PMMA has the possibility to make the POF amplifier and POF laser in the 648 nm wavelength region.

Table 3. Calculated emission cross-sections for three transitions of $Sm(DBM)_3Phen$-doped PMMA.

| Radiative transition | Transition wavelength (nm) | Emission cross-section ($cm^2$) |
|---|---|---|
| $^4G_{5/2} \rightarrow {}^6H_{9/2}$ | 648 | $2.11 \times 10^{-21}$ |
| $^4G_{5/2} \rightarrow {}^6H_{7/2}$ | 601 | $4.27 \times 10^{-22}$ |
| $^4G_{5/2} \rightarrow {}^6H_{5/2}$ | 566 | $4.56 \times 10^{-23}$ |

In conclusion, the optical properties of the $Sm^{3+}$ ion in the $Sm(DBM)_3Phen$-doped PMMA have been studied. The optical intensity parameters were calculated by using the absorption spectrum. The radiation lifetime of the $^4G_{5/2}$ metastable state, the stimulated emission cross-sections $\sigma_{ij}$ and the fluorescence branch ratios for $^4G_{5/2} \rightarrow {}^6F_{J'}$ and $^4G_{5/2} \rightarrow {}^6H_{J'}$ are also evaluated. The radiation transition probability of the $Sm^{3+}$ ion in the PMMA shows that $Sm(DBM)_3Phen$-doped PMMA is efficient for laser excitation, which is promising for making polymer optical active devices.

# References


[1] Kuriki K, Nishihara S, Nishizavva Y, Tagaya A, Okamoto Y and Koike Y 2001 *Electron. Lett.* **37** 415

[2] Yang B, Ming H, Zhang Q J and Xie J P 1998 *Chin. Phys. Lett.* **15** 272

[3] Guo Y, Bai M, Tang L and Ming H 2002 *Chin. Phys. Lett.* **19** 1369

[4] Zheng Z Q, Ling H, Ming H, Zhang Q J, Chen B, Sun X H and Xie J P 2003 *Chin. Phys. Lett.* **20** 654

[5] Zhang Q J, Wang P, Sun X F, Zhai Y, Dai P, Yang B, Ming Hai and Xie J P 1998 *Appl. Phys. Lett.* **72** 407

[6] Kobayashi T U, Nakatsuka S, Iwafuji T, Kuriki K, Imai N and Yamamoto T 1997 *Appl. Phys. Lett.* **71** 2421

[7] Judd B R 1962 *Phys. Rev.* **127** 750

[8] Ofelt G S 1962 *J. Chem. Phys.* **37** 511

[9] Wang G 2001 *J. Opt. Soc. Am.* B **18** 173

[10] Guo Y, Zheng X, Ming H and Zhang Q J 2001*Chin. Phys. Lett.* **18** 1337

[11] Xu X S, Ming H and Zhang Q J 2001*Opt. Commun.* **199** 369

[12] Koeppen C, Yamada S, Jiang G and Garito A F 1997 *J. Opt. Am. Soc.* B **14** 155

[13] Melby L R, Rose N J, Abramson E and Caris J C 1964 *J. Am. Chem. Soc.* **86** 5117

[14] Krupke W F 1974 *IEEE J. Quantum Electron.* **10** 450

[15] Carnall W T, Fields P R and Rajnak K 1965 *J. Chem. Phys.* **42** 3797

[16] Farries M C, Markel P R and Townsend J E 1988 *Electron. Lett.* **24** 709